Department of Biochemical Engineering and Biotechnology

Indian Institute of Technology Delhi

Sensitivity of Choice of Sectoral Model on Bacterial Growth Analysis

Guided by: **Prof. Anjan Roy**

Submitted by: **Prathamdeep Dhanoa** (2021BB10005)

November, 2024

Contents

List of Figures

List of Abbreviations/Symbols

- PTR - Precursor-Transporter-Ribosome Model.
- PTRWF - Precursor-Transporter-Ribosome-Regulatory Molecule-Internal Food Model
- f_R - Fraction of Ribosomes allocated to Ribosomal Proteins.
- f_T - Fraction of Ribosomes allocated to Transporter Proteins.
- μ - Balanced Exponential Growth Rate.
- f_R - Fraction of Ribosomes allocated to Ribosomal Proteins.
- m_R - Number of P monomers used in making R(Ribosome).
- m_T - Number of P monomers used in making T(Transporter Molecule).
- P, T, R, W, F - Respective population of each species.
- k - Translational Efficiency(peptide elongation rate of a ribosome per unit concentration of P)
- v_P, v_T, v_R, v_W, v_F - Volume occupied by a single respective species' molecule.
- $[F_e]$ - External substrate(food) concentration
- h_W - Hill function encapsulating the P dependence of W.
- d_R, d_T - Rate of degradation of R and T in the cytosol, respectively.
- $\theta_T, \theta_R, \theta_W, k_P, k_W, k_F$ - Parameters of the model.
- Θ_R - Mass fraction of ribosomes relative to total protein pool.
- q - Medium quality.
- CB, NCB, NCNB, CNB - Cost/Benefit regimes of the PTRWF model.

1 Abstract

Modelling bacterial physiology through sectoral models that reproduce the bacterial growth laws is an active area of research. Incrementally increasing the complexity of the models helps us find the limitations and advatages that each layer of complexity adds. This report capitulates an attempt to analyse a simple P-T-R model, building on to the P-T-R-W-F model which models the translational regulation via the Stringent Response. We find that incorporating regulation, when considered with its costs and benefits, is not always beneficial in stable environments, however, it confers considerabe advantage to cells in fluctuating environments in the long run.

2 Introduction

2.1 Background

2.1.1 Golden Age of Bacterial Growth Laws(1950s)

The 1950s marked a transformative period in bacterial physiology, often referred to as the "Golden Age of Bacterial Growth Laws." This era was characterized by significant advancements in understanding the quantitative aspects of microbial growth, largely driven by the pioneering work of Jacques Monod. Monod's introduction of the Monod equation in 1949 was a seminal breakthrough that provided a mathematical model to describe the relationship between microbial growth rates and substrate concentration, analogous to enzyme kinetics described by the Michaelis-Menten equation [1]. This model became foundational in microbiology and environmental engineering, particularly in applications like wastewater treatment, where understanding microbial growth dynamics is crucial.

Monod's work laid the groundwork for a more systematic exploration of bacterial growth, emphasizing the importance of substrate concentration as a limiting factor for microbial proliferation. The Monod equation introduced key parameters such as the maximum specific growth rate ($\mu_{\max}$) and the half-saturation constant (K_s), which describe how efficiently microorganisms utilize substrates under varying conditions [1]. These parameters allowed researchers to predict and manipulate microbial behavior in both natural and engineered systems.

During this golden age, the concept of balanced growth also emerged as a critical framework for studying bacterial physiology. Balanced growth refers to a steady state where all cellular components grow at constant rates, maintaining proportionality throughout the cell cycle [2]. This concept was crucial for understanding how bacteria adapt to changes in environmental conditions and nutrient availability. Researchers like Ole Maaløe and Niels Kjeldgaard further explored these ideas, investigating how macromolecular synthesis is regulated during different growth phases [3].

Moreover, this period witnessed a shift towards integrating molecular biology with bacterial physiology. The insights gained from studying bacterial growth kinetics informed broader research into gene regulation and metabolic pathways. Monod himself later contributed significantly to the field of molecular biology, particularly through his work on gene expression regulation, which earned him a Nobel Prize in 1965 alongside François Jacob and André Lwoff [4].

Overall, the 1950s were pivotal in establishing a quantitative foundation for bacterial physiology. The innovations of this era not only enhanced our understanding of microbial growth dynamics but also set the stage for future research into microbial ecology and biotechnology. The principles developed during this time continue to influence contemporary studies on microbial metabolism and environmental microbiology, demonstrating the enduring impact of this golden age on the field.

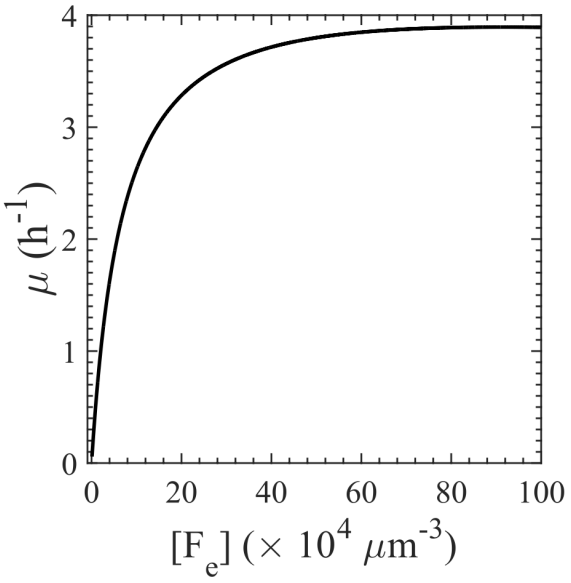

Figure 1: Monod's Growth Law, as reproduced through simulations by [7]

2.1.2 Growth Laws after Monod

Following Monod's groundbreaking work in the 1940s and 1950s, the study of bacterial growth laws evolved significantly, particularly in understanding the relationship between ribosomal mass fraction and growth rate in varying environments. The linear relationship between ribosomal content and growth rate was initially observed by Schaechter et al., who noted that the RNA/protein ratio, a proxy for ribosomal mass fraction, is directly proportional to the growth rate during balanced exponential growth [5]. This finding was pivotal as it linked the cellular machinery for protein synthesis directly to the physiological state of the cell. As ribosomes are primarily composed of ribosomal RNA (rRNA), which constitutes about 85% of total RNA in *E. coli*, this relationship highlighted the critical role of ribosomes in determining growth rates.

Subsequent studies by Neidhardt and Magasanik further cemented this relationship, showing that changes in nutrient quality lead to adjustments in ribosomal content, thereby modulating growth rates [6]. This linear correlation is understood as a consequence of mass balance, where protein synthesis is driven by elongating ribosomes. In balanced growth conditions, this results in a direct proportionality between ribosomal mass fraction and growth rate. The constant of proportionality is determined by the reciprocal of the translational elongation rate, indicating that faster translation allows for higher growth rates.

Recent research has continued to explore this relationship, particularly focusing on how environmental changes affect ribosomal abundance and activity. Studies have shown that as nutrient quality improves, both the growth rate and ribosomal mass fraction increase [8]. This is because better nutrient conditions allow for more efficient protein synthesis, necessitating an increase in ribosome numbers to meet the demands of rapid cell growth. However, this linear relationship holds primarily for moderate to fast growth rates; at very low growth rates,

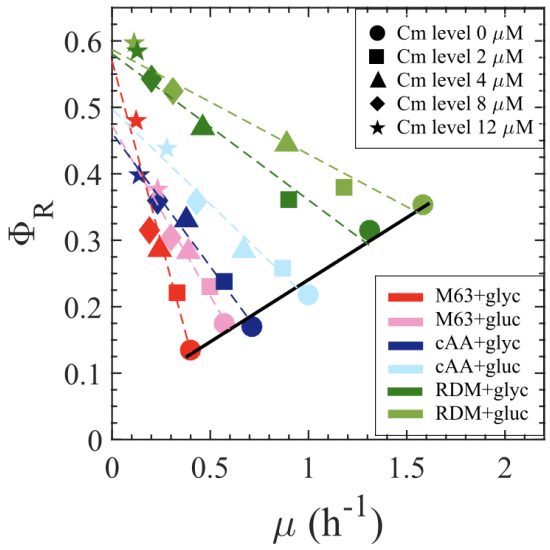

Figure 2: Bacterial Growth Laws with Varying Medium Quality/Richness, F_e and Translational Efficiency, k [7]

deviations occur due to limitations in translation elongation rates and resource allocation.

2.2 Literature survey

Sectoral models have emerged as an important approach for understanding bacterial growth and resource allocation. These models divide the bacterial proteome into distinct functional categories or ”sectors”, typically including ribosomal, metabolic, and housekeeping proteins. The key idea is to examine how bacteria optimize the allocation of proteomic resources between these sectors under different environmental conditions. Key developments in sectoral models include proteome partitioning constraints, as demonstrated by Scott et al. [9, 10]. They showed that the allocation of cellular resources between different proteome sectors is subject to constraints, leading to trade-offs in gene expression. Notably, they found that the ribosomal protein fraction exhibits a linear relationship with growth rate when nutrient quality is varied. The work on proteome sectors has helped explain the empirical bacterial ”growth laws” first observed by Schaechter, Maaløe and Kjeldgaard in the 1950s. These laws describe how cell size and composition vary with growth rate under different nutrient conditions. Researchers have developed coarse-grained models that focus on a few key proteome sectors rather than detailed molecular mechanisms. This simplification allows for analytical solutions and broader insights into resource allocation strategies. Many sectoral models assume that bacteria allocate resources to optimize growth rate. This optimization approach has been successful in reproducing observed patterns of proteome allocation. Models have also incorporated regulatory mechanisms like ppGpp-mediated stringent response to explain how bacteria dynamically adjust proteome allocation in response to environmental changes. Recent work has examined the costs and benefits of regulation in sectoral models, including analyzing the burden of produc-

ing regulatory molecules versus the growth advantage they provide. While early work focused on steady-state growth, more recent models have examined proteome allocation in fluctuating environments. Advances in proteomics and single-cell measurements have allowed for better quantification of proteome sectors, enabling more rigorous testing of model predictions. Key papers in the development of sectoral models include Scott et al. [9], which introduced the proteome sector model and growth laws. You et al. [11] extended the sector model to include a "constant" proteome fraction. Hui et al. [12] provided experimental support for proteome sectors using ribosome profiling. Giordano et al. [13] developed a minimal model of proteome allocation. Jain et al. [14] analytically derived growth laws from a simple sectoral model. They later examined cost-benefit tradeoffs in regulated versus unregulated models[7]. In this thesis, we aim to analyse sectoral models by gradually increasing complexity and then comparing their limitations and advantages.

2.3 Objectives

1. To understand and validate the sectoral model proposed by Jain et al by gradually increasing complexity
2. To find an alternative relation for regulation by regulator molecules by varying the hill's coefficient in the equation relating f_R and W.
3. To propose an alternate paradigm for regulation within the PTRFW model that more closely resembles the stringent response.
4. Compare transient responses of regulation with time for different models.
5. Using Jain et al(2018) as a starting point, to relate and compare other sectoral models, such as the one formulated by Roy et al to ascertain sensitivity of choice of model for growth laws.
6. Incorporate stochastic modelling in ribosome population count to better model realistic conditions.

3 Methods

3.1 Model

3.1.1 P-T-R Model (Jain *et al.*, 2016 [14])

The 'Precursor-Transporter-Ribosome' model is perhaps the simplest of all sectoral models. It trifurcates the protein pool into three parts:

1. **Precursor:** This pool contains all the amino acids precursors that are part of the total protein mass of the cell.

2. **Transporter:** Transporters are the metabolic proteins that convert all food molecules into precursors and also transport them within the cell, leading to uptake of exernal food substrate.

3. **Ribosome** represents the number of ribosomes in the cell.

The equations describing the model are as follows:

$$\frac{dP}{dt} = K_P T - k\frac{RP}{V} \tag{1}$$

$$\frac{dR}{dt} = \frac{kf_R RP}{m_R V} - d_R R \tag{2}$$

$$\frac{dT}{dt} = \frac{kf_T RP}{m_T V} - d_T T \tag{3}$$

$$K_P = k_P q \tag{4}$$

The following image capitulates the above set of ODEs [14]:

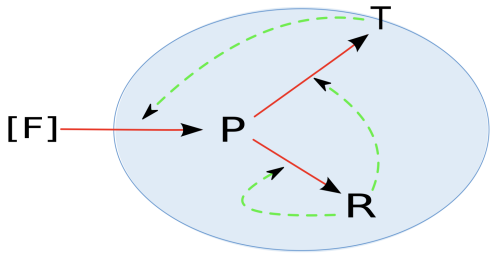

Figure 3: The PTR cell. Precursor molecules (P) are produced by the catalytic action of the metabolic proteins (T) on the external food molecules (F). Metabolic proteins and ribosomal proteins (R) are synthesized from the P molecules in reactions catalysed by R

3.1.2 P-T-R-W-F Model(Jain *et al.*, 2018 [7])

The PTRWF model is a more elaborate system of ODEs that models the cost and benefit on metabolism by regulation, The model incorporates a more realistic mechanism of translational regulation, called the Stringent Response, which decreases protein production by the recruitment of regulatory molecules such as ppGpp, RelA, SpoT to the ribosome in the presence of uncharged t-RNA strands.
Two notable additions from the previous PTR model are as follows:

1. **Regulatory molecule(ppGpp) or W:** This is the number of ppGpp molecules in the cell.

2. **Internal Food or F:** The number of food molecules internalised from external substrate by T.

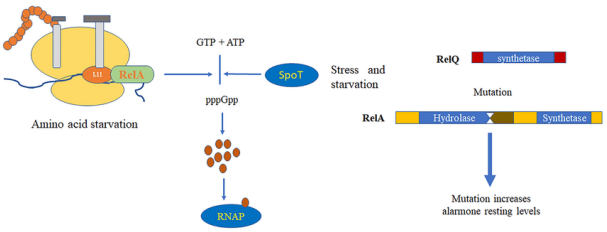

Figure 4: The stringent response inhibition mechanism involving the presence of the alarmone, ppGpp [15]

The equations describing the model are as follows:

$$\frac{dP}{dt} = K_P T - k\frac{RP}{V} \tag{5}$$

$$\frac{dT}{dt} = \frac{k f_T RP}{m_T V} \tag{6}$$

$$\frac{dR}{dt} = \frac{k f_R RP}{m_R V} \tag{7}$$

$$\frac{dW}{dt} = K_W T h_w \tag{8}$$

$$K_P = k_P \frac{F}{V}; K_W = k_W \frac{F}{V} \tag{9}$$

$$f_R = \left(\frac{\theta_R}{\theta_R + \frac{W}{V}}\right); f_T = \left(\frac{\frac{W}{V}}{\theta_T + \frac{W}{V}}\right) \tag{10}$$

$$h_w = \left(\frac{\theta_w}{\theta_w + \frac{P}{V}}\right) \tag{11}$$

$$K_f = k_f[F_e] \tag{12}$$

$$\frac{dF}{dt} = K_F T - K_P T - K_W T h_w \tag{13}$$

Here we see a more elaborate set of ODEs that define the system, with regulation included via f_R and f_T. Where we see that increasing the regulatory molecule(W), decreases f_R, here, it is assumed that $\theta_R = \theta_T$. This leads to

$$f_R + f_T = 1 \tag{14}$$

The volume is modelled proportional to the populations of all species,

$$V = v_P P + v_T T + v_R R + v_W W + v_F F \tag{15}$$

Cell division is taken to follow the sizer model wherein the cell divides upon reaching the critical volume $V_c = 1\mu\text{m}^3$. This is modelled by instantaneous halving of all species' populations as soon as V reaches V_c. The image below from [7] capitulates the essence of the PTRWF model:

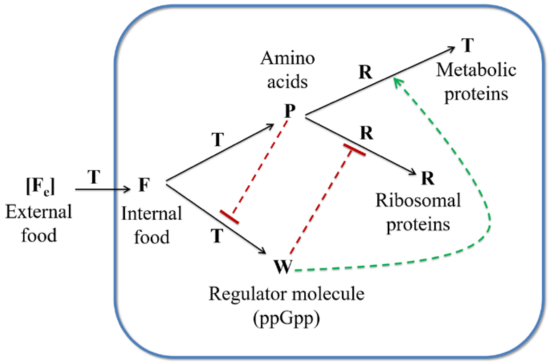

Figure 5: Schematic of the model indicating the reactions (solid arrows), catalysts (symbols over solid arrows) and regulatory links (dashed lines).

3.1.3 Min() Model(Roy *et al.*, 2021)

The model presents a unified autocatalytic network framework with three coupled cycles: ribosome, RNA polymerase, and tRNA charging cycles. The core transcription-translation machinery self-replicates through these interconnected cycles, each generating two types of growth laws.

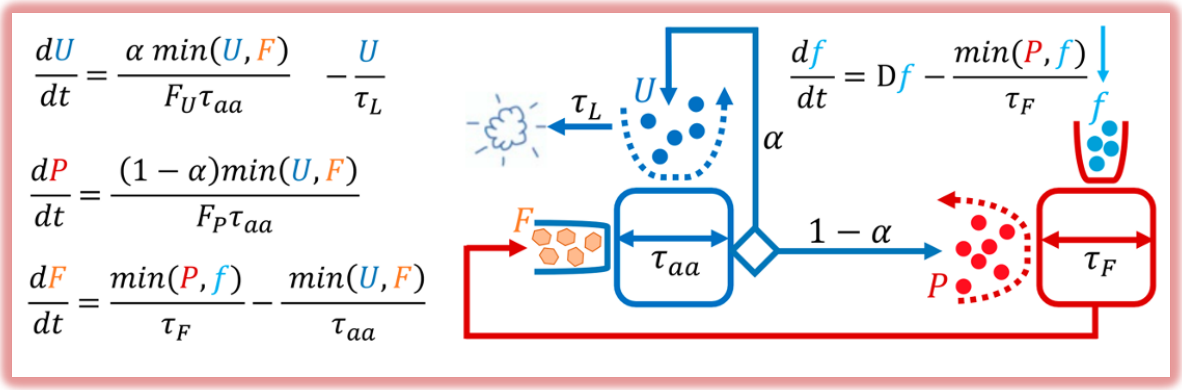

Figure 6: The min(UPF) model as proposed by Roy et al., 2021

The ribosome cycle is governed by:

$$\left(\mu\tau_{\text{SA}(R)} + 1\right)\left(\mu\tau_{\text{pool}(RP_j)} + 1\right)\left(\mu + \frac{1}{\tau_{\text{life}(R)}}\right) = \frac{\alpha_{RP_j}}{\tau_{RP_j}}\frac{R_b}{R}$$

where:

- μ is growth rate
- τ parameters represent various timescales
- α represents allocation parameters

The RNA polymerase cycle follows:

$$\prod_{i=1}^{4}(1+\mu\tau_i) = \frac{\tau_{\text{life}(Rpol)}\alpha_{rpo_j}R_{m(Rpo_j)}\tau_{\text{life}(m(Rpoj))}}{\tau_{Rpo_j}\tau_{rpo_j}}\tilde{\phi}_b$$

These cycles are coupled because:

- Ribosomes require RNA polymerase to transcribe rRNA
- RNA polymerase requires ribosomes to translate rpo genes

The model demonstrates how these coupled cycles achieve balanced exponential growth without complex feedback mechanisms. Each cycle generates:

- Relative abundance laws relating growth rate to catalyst fractions
- Closed-cycle laws connecting growth rate to all timescales within a cycle

This framework explains how perturbations in one cycle affect others and predicts growth behavior under various conditions, including temperature changes and antibiotic treatments.

3.2 Softwares and Packages

All simulations were run on Python3.12 and implemented in the VSCode IDE. Python was chosen for its robust scientific libraries and ease of use for numerical simulations.

- Python Libraries Used:
  - NumPy: For handling arrays and performing numerical computations.
  - SciPy: Specifically, the `odeint` function from the SciPy library was used to solve the system of ordinary differential equations (ODEs)
  - Matplotlib: For visualizing the results of the simulations and plotting the growth curves and other relevant data.

3.3 Parameter Values

3.3.1 From Figure 6 to Figure 9

- $k_P = 250\text{h}^{-1}\,\mu\text{m}^3$
- $d_T = 0.1\,\text{h}^{-1}\,\mu\text{m}^3$
- $d_R = 0\,\text{h}^{-1}\,\mu\text{m}^3$

- $m_T = 500$
- $m_R = 10000$
- $k = 5 \times 10^{-4}\,\mathrm{h}^{-1}\,\mu\mathrm{m}^3$
- $v_P = v_T = v_R = v_W = v_F = v = 10^{-8}\,\mu\mathrm{m}^3$
- $V_c = 1\,\mu\mathrm{m}^3$

3.3.2 From Figure 10 to Figure 15

- $k_F = 0.04\,\mathrm{h}^{-1}\,\mu\mathrm{m}^3$
- $[F_e] = 6 \times 10^4\,\mu\mathrm{m}^{-3}$
- $k_P = 5 \times 10^{-3}\,\mathrm{h}^{-1}\,\mu\mathrm{m}^3$
- $k_W = 10^{-3}\,\mathrm{h}^{-1}\,\mu\mathrm{m}^3$
- $m_T = 500$
- $m_R = 10000$
- $k = 5 \times 10^{-4}\,\mathrm{h}^{-1}\,\mu\mathrm{m}^3$
- $\theta_T = \theta_R = \theta = 2 \times 10^7\,\mu\mathrm{m}^{-3}$
- $\theta_W = 10^7\,\mu\mathrm{m}^{-3}$
- $v_P = v_T = v_R = v_W = v_F = v = 10^{-8}\,\mu\mathrm{m}^3$
- $V_c = 1\,\mu\mathrm{m}^3$

3.4 Initial Values

```
P0 = 1e4
R0 = 1e4
T0 = 1e4
W0 = 1e4
F0 = 1e4
```

4 Results and Discussions

The PTR model(with optimisation assumption) and the PTRWF model show exponential balanced growth rate(Figure 6, Figure 10). Incorporation of Division(sizer model) is also given below in Figure 7. A response similar to found in the PTRWF model(Figure 11)

One thing to note is that the PTR model as of yet does not simulate the Monod's equation, but by the *Optimisation Algorithm*, first employed by Molenaar et al [16] was implemented by [14], where the optimal f_{Ropt} was calculated for each q value. Using these f_{Ropt} reproduced the Monod's Law and the other Growth Laws as was found by [14]. To simulate cell division in accordance with the sizer model, populations were halved as soon as the volume exceeded Vc. The gradients were calculated from the slope of the upward part of the curve for μ calculation(Figure 7, Figure 11).

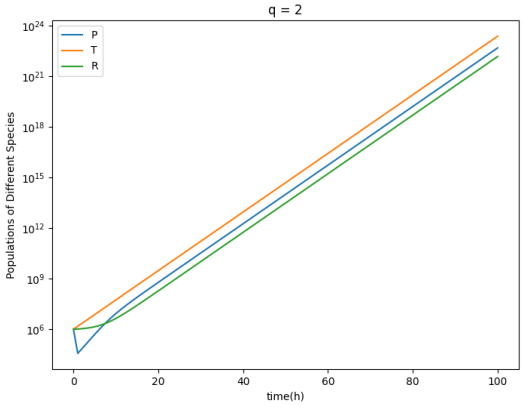

Figure 7: A log-linear plot shows the balanced growth condition satisfied by the PTR model without accounting for division. The initial transient can be explained by the sudden depletion of P by T and R and the corresponding increase once KpT becomes significant.

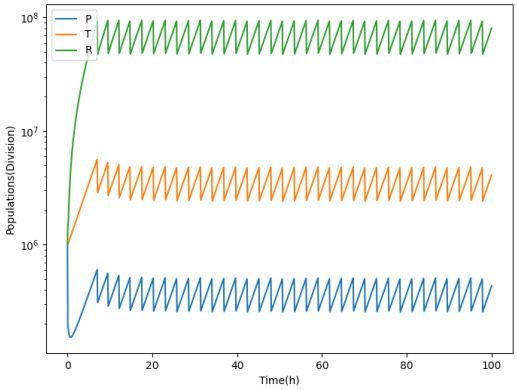

Figure 8: The same log linear plot when accounting for division via the sizer model choosing a critical volume of Vc = 1 μm^3.

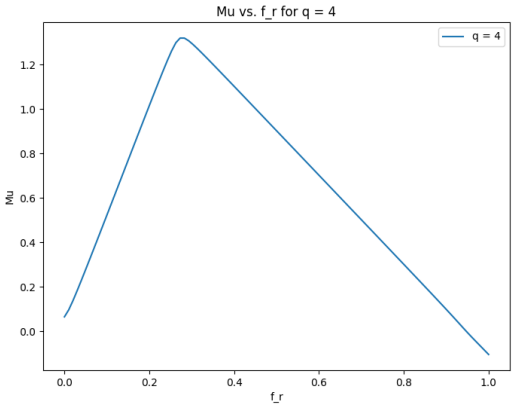

Figure 9: Calculating f_{Ropt} for a single q values to be used in place of regulation in the PTR model under the optimisation assumption.

Simulating the *Optimisation Assumption* as a proxy for regulation, f_{Ropt} value for a specific q value can be calculated from the peak of the triangular curve.

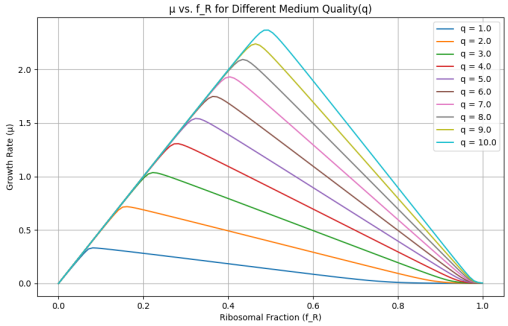

Figure 10: μ vs f_R for different q values

The same plotting when carried out for different values of q is plotted in Figure 9. The graph shows the adjustments made by the cell in different environments. Generally speaking, increasing the richness of the media(q)increases f_R.

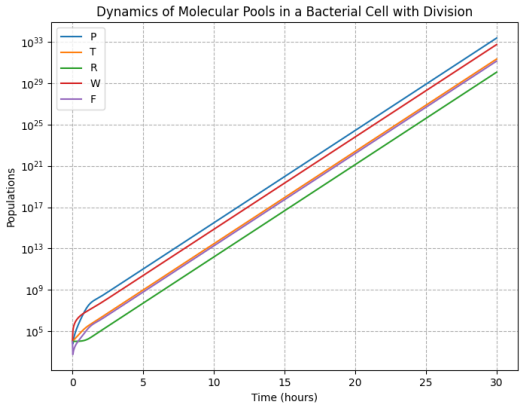

Figure 11: Balanced exponential growth of all species shown by PTRWF model; log-linear plot yields a straight line.

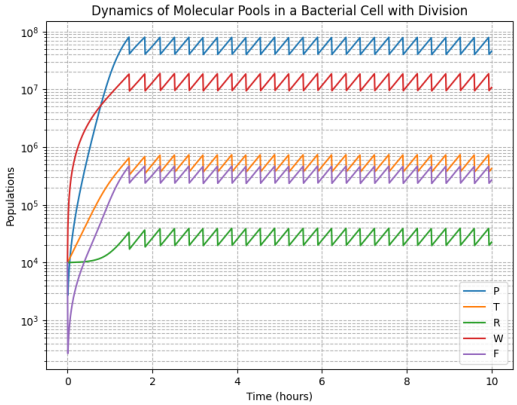

Figure 12: Growth of populations when accounting for division(sizer model applied similar to implementation in PTR model)

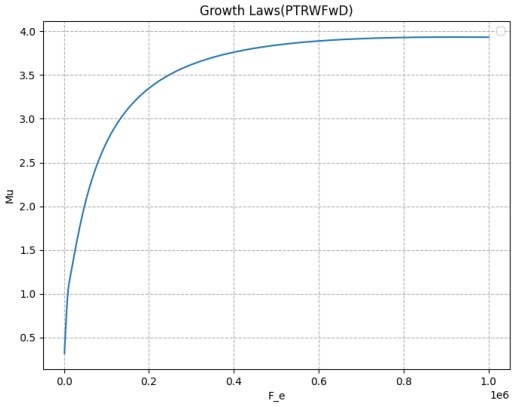

Figure 13: μ vs. F_e as derived from simulation of the model. The model qualitatively resembles the Monod kinetics after considering cost and benefits of regulation.

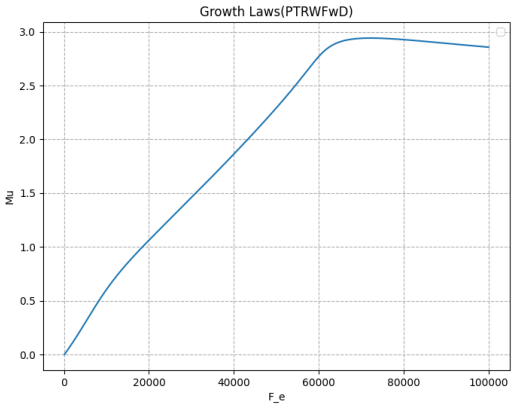

Figure 14: μ vs. F_e without accounting for the cost and benefit of the PTRWF model(NCNB); $k_W = 0$ and $f_R^* = 0.4915$

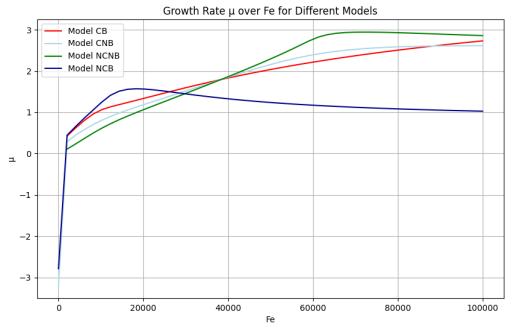

Figure 15: μ vs. F_e for different cost and benefit paradigms- CB, NCNB, CNB, NCB. The graphs have not yet been fully replicated and are still in the debugging phase.

Although the graphs of CNB and NCB are yet to be properly reproduced, plots of CB and NCNB have been properly plotted. Figure 14 shows that incorporating regulation is not always advantageous as the two graphs intersect each other at two points L and U, between which the NCNB is better than CB.

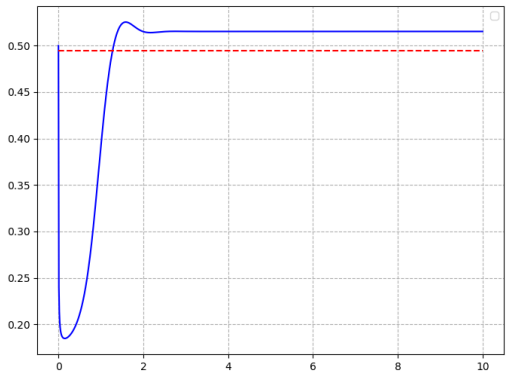

Figure 16: f_R vs. $time(h)$ showing the transient response of regulation of f_R. The red-dashed line corresponds to $f_R^* = 0.4915$. Final steady state value of $f_{Rss} = 0.5151$.

The transient response in reaching the steady state is of particular interest, as a faster response confers specific advantage to the cell in presence of varying external conditions. Figure 15 shows the transient response of f_R before reaching steady state. For the PTR model, due to its nature, it is not possible to have a transient analysis of this sort since f_R in that case is calculated through optimisation which only gives a steady state value.
Figure 16 shows the comparison between CB and NCNB in fluctuating environment conditions, with the regulated model(CB) faring better than the unregulated model(NCNB). Showing that regulation confers its advantage specifically in form of the speed of response in a changing environment.

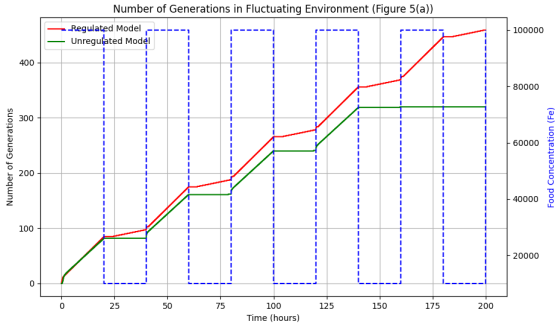

Figure 17: Comparison of CB and NCNB for a fluctuating environment F_e; n is the number of generations w.r.t time(h)

4.1 Employing the min() methodology

The PTRWF model does not consider nutrient-starved conditions which a cell might encounter. The autocatalytic min(.) model proposed by Roy et al. in 2021 could potentially lead to a more realistic behaviour which a growing cell is likely to follow in a nutrient-starved condition.
The results from the min(.) model implementation are as follows:

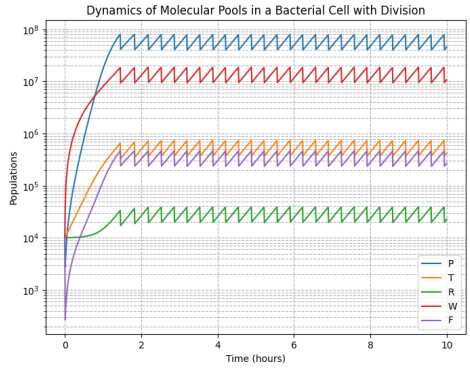

(a) Original PTRWF

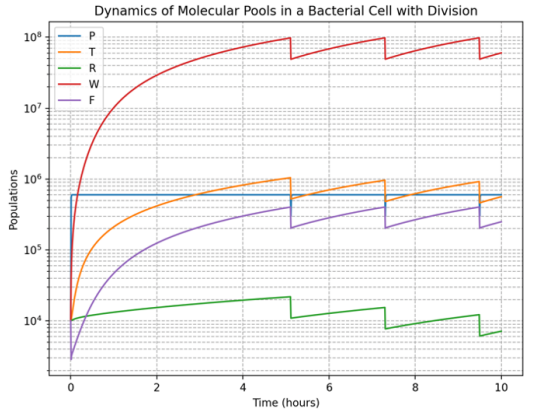

(b) Modified PTRWF

Figure 18: The slope is less steeper in the log(Population) vs t graph, indicating that μ is lesser than the original PTRWF model.

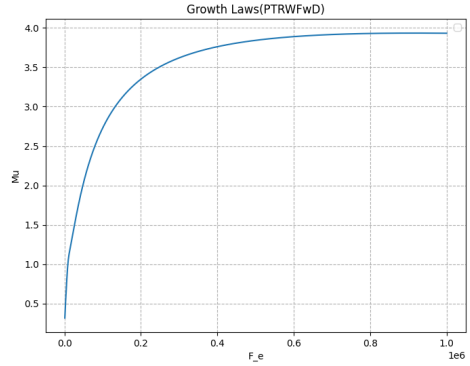

(a) Original PTRWF

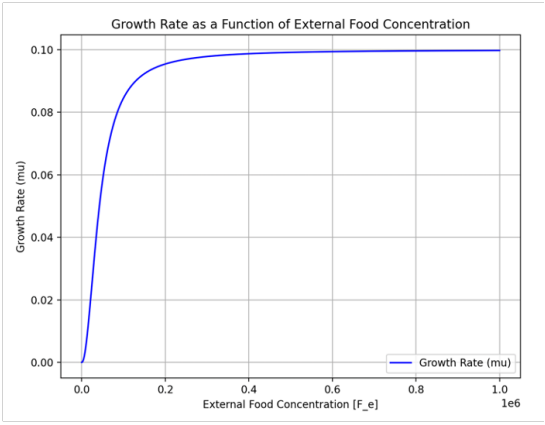

(b) Modified PTRWF

Figure 19: The Monod Kinetic graphs are different with the modifications in PTRWF model. Worth noting is the very low value of μ at nutrient saturation, indicating that the modification doesn't suit nutrient rich media and substrate prioritisation occurs at the cost of growth.

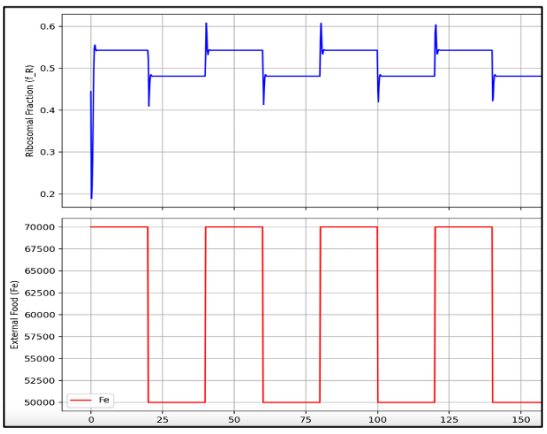

(a) Original PTRWF

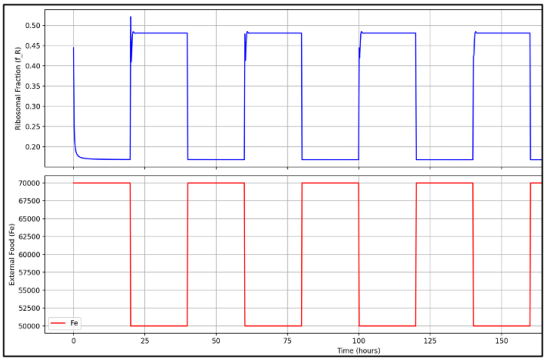

(b) Modified PTRWF

Figure 20: Our modification, although devastating to the growth rate in most conditions, renders the cell some evolutionary advantage in a medium switching from high to low value in a square-wave manner, the frequency of which corresponds with that shown by f_R. The cells undergoing our modification in the lower food regime undergo better stability response to external sudden changes over time.

5 Future Work

1. Validating the paradigm with existing literature and comparing with other models.
2. Incorporating bacterial energetics via ATP allocation to further strengthen the model.
3. Comparison of response times and transient analysis across different sectoral models.
4. Using more realistic parameters using data from Dennis and Bremmer(1995), Scott et al.(2010) and other seminal experiments to make the data fit for comparison with other models.

6 References

[1] Jacques Monod. "The Growth of Bacterial Cultures". In: *Annual Review of Microbiology* 3 (1949), pp. 371–394.

[2] Moselio Schaechter, Ole Maaløe, and Niels O. Kjeldgaard. "Dependency on Medium and Temperature of Cell Size and Chemical Composition during Balanced Growth of Salmonella typhimurium". In: *Journal of General Microbiology* 19 (1958), pp. 592–606.

[3] Ole Maaløe and Niels Ole Kjeldgaard. *Control of Macromolecular Synthesis*. New York, NY: W. A. Benjamin, 1966.

[4] Jacques Monod, François Jacob, and André Lwoff. *Nobel Prize in Physiology or Medicine 1965*. https://www.nobelprize.org/prizes/medicine/1965/summary/. 1965.

[5] Moselio Schaechter, Ole Maaløe, and Niels O. Kjeldgaard. "Dependency on Medium and Temperature of Cell Size and Chemical Composition during Balanced Growth of Salmonella typhimurium". In: *Journal of General Microbiology* 19 (1958), pp. 592–606.

[6] Frederick C. Neidhardt and Boris Magasanik. "Studies on the Role of Ribosomes in Bacterial Growth". In: *Biochimica et Biophysica Acta* 76 (1963), pp. 448–462.

[7] Piyush P Pandey and Sanjay Jain. "Growth laws for cell populations in a minimal model of chemical dynamics". In: *Physical Biology* 15.5 (2018), p. 056002. DOI: 10.1088/1478-3975/aabe43.

[8] Hans Bremer and Patrick P. Dennis. *Modulation of Chemical Composition and Other Parameters of the Cell by Growth Rate*. Ed. by Neidhardt FC et al. American Society for Microbiology Press, 1996.

[9] Matthew Scott et al. "Interdependence of cell growth and gene expression: origins and consequences". In: *Science* 330.6007 (2010), pp. 1099–1102.

[10] Matthew Scott et al. "Emergence of robust growth laws from optimal regulation of ribosome synthesis". In: *Molecular systems biology* 10.8 (2014), p. 747.

[11] Chongzhao You et al. "Coordination of bacterial proteome with metabolism by cyclic AMP signalling". In: *Nature* 500.7462 (2013), pp. 301–306.

[12] Sheng Hui et al. "Quantitative proteomic analysis reveals a simple strategy of global resource allocation in bacteria". In: *Molecular systems biology* 11.2 (2015), p. 784.

[13] Nils Giordano et al. "Dynamical allocation of cellular resources as an optimal control problem: novel insights into microbial growth strategies". In: *PLoS computational biology* 12.3 (2016), e1004802.

[14] Piyush P. Pandey and Sanjay Jain. “Analytic derivation of bacterial growth laws from a simple model of intracellular chemical dynamics”. In: *Theory in Biosciences* 135.3 (2016), pp. 121–130. DOI: 10.1007/s12064-016-0227-9.

[15] Piyush P. Pandey and Sanjay Jain. “A minimal model of bacterial growth: coupling between cellular and population dynamics”. In: *Archives of Microbiology* 204.3 (2022), p. 176. DOI: 10.1007/s00203-022-02776-2.

[16] Evert Bosdriesz et al. “How fast-growing bacteria robustly tune their ribosome concentration to approximate growth-rate maximization”. In: *FEBS Journal* 282.10 (2015), pp. 2029–2044. DOI: 10.1111/febs.13258.